Available online at www.sciencedirect.com
ScienceDirect
Solar Energy Materials & Solar Cells 92 (2008) 736–745
Solar Energy Materials and Solar Cells
www.elsevier.com/locate/solmat

A setup for studying stability and degradation of polymer solar cells

Suren A. Gevorgyan, Mikkel Jørgensen, Frederik C. Krebs*

National Laboratory for Sustainable Energy, Technical University of Denmark, Frederiksborgvej 399, DK-4000 Roskilde, Denmark

Received 13 November 2007; received in revised form 14 February 2008; accepted 14 February 2008

Abstract

A detailed description of a setup for studying ageing of polymer devices is presented. The system offers individual control of the environmental factors (oxygen, humidity, atmosphere, temperature and light intensity) causing the degradation of organic devices. The system was developed for accurate control of the conditions and data collection of photovoltaic (PV) parameters for organic solar cells during long-term testing. The atmosphere chamber can operate under vacuum conditions without temperature control. It is designed for operation at an internal gas pressure of around 1 atm. It is further equipped for isotopic labeling experiments of the internal atmosphere ($^{18}O_2$ and $H_2{}^{18}O$) such that degradation mechanisms can be studied using TOF-SIMS as a chemical probe. Experiments on both "accelerated" (by applying thermal stress to the devices) and "long-term" lifetime measurements of traditional organic bulk heterojunction solar cell devices have been realized while controlling the environmental conditions. As an example of use of the setup we determined the acceleration factor for standard bulk heterojunction devices based on ITO/PEDOT:PSS/P3HT-[60]PCBM/Al when operated under an ambient atmosphere and under an inert atmosphere at temperatures of 25, 43, 63 and 83 °C. Different values for the acceleration factor were found depending on the atmosphere used and further our results suggest that the acceleration factor may change in time as different degradation mechanisms may dominate at different times during the device life.

Keywords: Stability; Degradation; Accelerated testing; Multiple processes; Setup; Instrumentation

1. Introduction

The field of polymer solar cells is still in a state of rapid development and has been reviewed several times [1–8]. The efficiency has reached 5% for simple bulk heterojunction cells [9,10] and 6.5% for tandem cells [11], while theoretical predictions suggest that it should be possible to obtain 10% [12,13]. The short operational stability and lifetime still remain one of the key issues of polymer PVs [14]. Significant improvement of stability and increase of lifetimes up to scales that could comply with industrial standards are essential requirements for further progress and commercialization of organic solar cell devices.

The ageing phenomenon in the organic solar cells occurs due to the combined influence of environmental factors, such as light, temperature, oxygen, humidity and intrinsic factors such as the constituents of the device. A number of scenarios have been proposed to describe the degradation processes [15–26] mainly using TOF-SIMS [20–26]. As yet, however, there is no general rule as to what mechanisms take place for any given device disposition and each case must still be studied in detail and while some basic mechanisms have been identified the overall scheme still remains unclear. In order to produce devices with good stability, it is necessary to thoroughly understand the decay mechanisms taking place in the cells. The effect of each of the aforementioned environmental components must be understood and mapped in order to prevent or sufficiently slow down the processes that they result in. Therefore, it is essential to develop an efficient procedure for accurate stability measurements of organic solar cell devices, while controlling all the affecting parameters individually. Methods, standards and equipment for studying inorganic solar cells were developed in the mid-1980s along with standardized measurement procedures of power conversion efficiency through a massive series of publications and standards [27–37] that later have been adapted for power

*Corresponding author. Tel.: +45 46 77 47 99.
E-mail address: Frederik.krebs@risoe.dk (F.C. Krebs).

0927-0248/$ - see front matter © 2008 Elsevier B.V. All rights reserved.
doi:10.1016/j.solmat.2008.02.008

conversion efficiency measurements of organic solar cells [38–40]. From this point of view one may ask why there is any need for a description of an apparatus for doing essentially the same with the exception that the solar cell is a polymer or an organic-based device. To answer this question we point to the fact that polymer and organic PVs differ from the inorganic technologies in the way they break down as detailed in this issue [14]. Inorganic solar cells are nearly all intrinsically stable from a chemical point of view and the materials will withstand illumination under intense sunlight in the ambient atmosphere indefinitely. Organic and polymer materials do not have this ability and will degrade over time. From this point of view the degradation of PV devices based on inorganic and organic materials share only some of the mechanisms associated with degradation (i.e. mechanical, encapsulant, electrical connections) but they do not share the internal instability of the material that organics have. As a result organic solar cells require special techniques for studying degradation and stability [14,20–26].

Standard test conditions have been proposed for accurate indoor determination of the power conversion efficiency of organic solar cell devices [38–40], which allow for an evaluation of the cells in a comparable manner. However, it is technically complicated to characterize the cells within a longer period, if the lifetimes extend far beyond a month. One of the proposed partial solutions is long-term out-door testing of the cells under real sun [41] which includes the effect of nighttime and different weather conditions. As such this gives essential information on how the solar cell would perform under real conditions. In our case the aim is to correlate the observed degradation to the well-defined conditions of the experiment (light intensity, atmosphere, etc.) and from this point of view the demand for reliable weather conditions in the particular region are too extreme and in-door measurements using accelerated conditions are best suited. Accelerated lifetime measurements have been reported [42,43] and simply involve the application of a certain stress to the cells that accelerates the decay processes inside the device. The prediction of an operational lifetime under normal conditions can ideally be predicted from the accelerated data and the acceleration factor assuming that it is constant. The acceleration factor may vary depending on the type of the material and conditions.

In this article we describe a setup that allows for controlled and accurate long-term stability measurements of organic PV devices. This easy-to-use setup consists of an atmospheric chamber (AC) (manufactured at the National Laboratory for Sustainable Energy) and apparatus for recording the decay of PV parameters. A full description of the AC that allows for creating specific environmental conditions during the testing process is given. A few words are devoted to installation of samples inside the chamber and realization of periodic lifetime measurements under certain ambient conditions. Additionally, to demonstrate the use of the apparatus we compare results of both accelerated and normal lifetime measurements for traditional polymer bulk heterojunction solar cells maintained under ambient or inert environmental conditions using the AC setup. The rates of degradation for the devices maintained under different conditions were used to estimate acceleration factors and the results are discussed.

2. Experimental

2.1. Description of the experimental setup

The general experimental setup is shown in Fig. 1. Up to two devices under investigation are placed in an AC beneath the sun simulator and connected to a source measure unit (SMU) through a multiplexing system (*vide supra*) to obtain diode characteristics at intervals. The intensity of the flux from the sun simulator is measured using a precision pyranometer (Eppley Laboratories) in conjunction with irradiance measurements using an optical spectrum analyzer (AvaSpec 2048 from Avantes) to ensure that the conditions approach AM1.5G. The solar simulator is Class AAA with the exception of the wavelength range 700–800 nm where it is Class AAB with respect to non-uniformity, temporal instability and spectral match. It is not possible to fit the pyranometer inside the chamber and therefore Hamamatsu S1133 KG5 filtered photodiodes were employed inside the chamber (see our website www.risoe.dk/solarcells for a routine solar simulator calibration). We have not corrected for mismatch in the data reported as the purpose is not accurate determination of the device efficiency but rather the relative degradation of the performance. It is however possible with the setup presented here and the standard method that has been

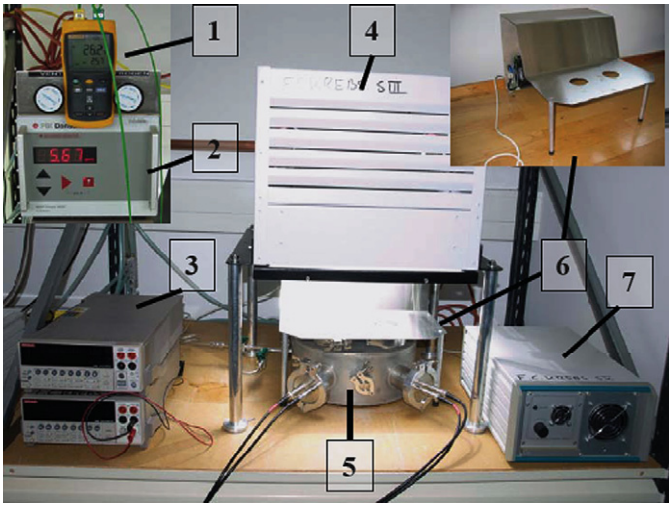

Fig. 1. *IV* testing setup: digital thermometer—to monitor the data of the thermocouples (1), O_2 Analyzer MAP Check 9000 (PBI Dansensor) (2), Keithley 2400 Sourcemeter and Keithley 2000 Multimeter—to transfer the *IV* data to PC (3), solar simulator (KHS Solar Constant 575) (4), atmospheric chamber (5), metal screen—to protect the chamber from overheating (also shown as an inset in the upper right corner) (6), power supply for solar simulator (7).

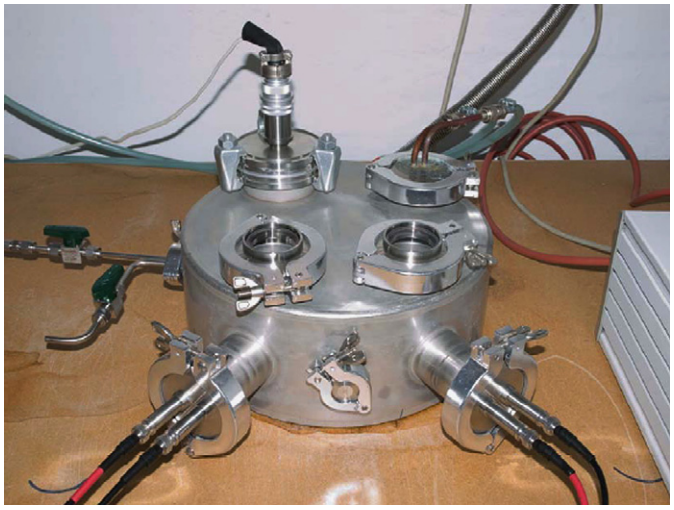

Fig. 2. General view of the atmospheric chamber (AC).

described in the literature [39,40]. A picture of the AC is shown in Fig. 2, and as a technical drawing in Fig. 3. The chamber is constructed as a closed steel cylinder with two access ports (flanges 6) for solar cell devices and corresponding viewports (Figs. 3 and 5)—quartz windows [44] mounted on the top. These windows have less than 10% absorbance in the wavelength range from 250 to 2600 nm and less than 50% up to 3400 nm. During measurements the chamber can be evacuated to remove any oxygen or water via flange (7) connected to an oil-free scroll-pump (vacuum: 10^{-2} mbar) or a turbomolecular pump (vacuum: $<10^{-6}$ mbar). Devices can also be measured in a controlled atmosphere e.g. nitrogen. This atmosphere (N_2 from a gas cylinder) is admitted through another flange (8). The ambient air is replaced by placing the entire chamber in a nitrogen-filled glove-box. If ambient or artificial atmosphere is present in the chamber inside fans are used to even out any temperature variations.

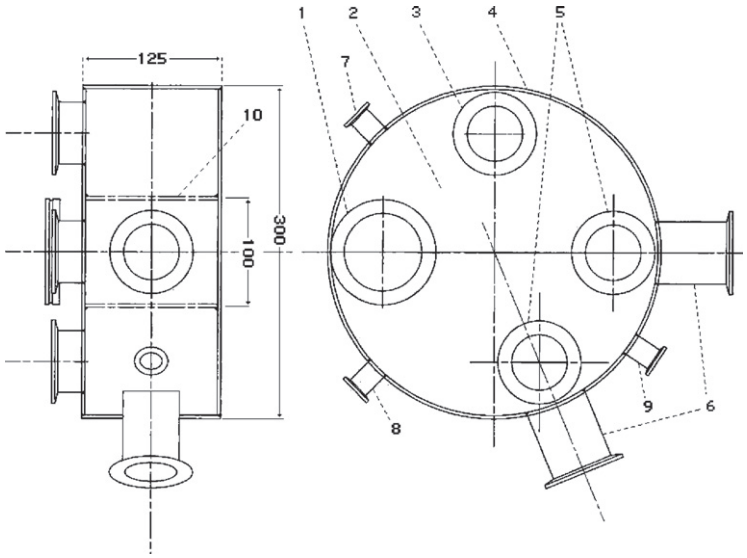

Item	Qty.	Description	Material	Purpose
1	1	DN63LF Flange	Stainless Steel	To introduce fans for circulation
2	1	Top Plate (thickness 3*)	Stainless Steel	-
3	1	KF50 Flange	Stainless Steel	To introduce cooling pipeline
4	1	Chamber Frame (thickness 3*)	Stainless Steel	-
5	2	KF50 Flange	Stainless Steel	Viewports for light exposure
6	2	KF50 Flange	Stainless Steel	To place testing samples
7	1	KF16 Flange	Stainless Steel	For Vacuum Pump and humidity sensor
8	1	KF16 Flange	Stainless Steel	To pump inert gases
9	1	KF16 Flange	Stainless Steel	To introduce thermocouples
10	1	Ring of central cylindrical cavity	Stainless Steel	-

*all dimensions are in mm

Fig. 3. Sketch of the atmospheric chamber: the side (left) and the top (right) views. All geometrical dimensions are in mm. Table below describes details of different components.

These fans are mounted through a large flange (1) shown in detail in Fig. 4a. The temperature affects both the performance and the lifetime of the devices so it must be controlled. This is achieved through active cooling with a cooling fluid circulating through copper pipes as shown in Fig. 4b. Some of the heat from the sun simulator can also be deflected using a metal screen so that light is only allowed through apertures over the windows in the chamber (upper right-hand inset in Fig. 1). External cooling fans are mounted on the backside of the screen so they can cool the chamber with the surrounding atmosphere. The parameters of temperature, pressure, oxygen and water content are measured using gauges and sensors. The temperature is measured with two thermocouples (type K) that go in through a flange (9). One is placed on a spring fixed on the bottom of the chamber directly under the device to be tested and another has thermal contact with the circulating atmosphere. The thermocouples are connected to an external multimeter (Fig. 1(1)) for read-out. A humidity sensor (Gallatec, CVC 2/5 humidity/temperature sensor) (Figs. 5 and 6) can be connected to the chamber using the flange for the vacuum pump, or via a T-shaped connector junction. In the latter case vacuum can be applied to the system while the humidity is measured. Another future possibility is to add a humidifier to the system to control the humidity over a range. The oxygen concentration inside the chamber is monitored using an O_2 analyzer (MAP Check 9000, PBI Dansensor) that is mounted on flange 8.

The solar cell devices are mounted on a sample holder that ensures the correct placement and orientation beneath the windows in the AC. A close-up is seen in Fig. 5. The sample holder consists of two copper rods with BNC connectors, one longer than the other, that are connected to the device using thermosetting silver epoxy paste. This holder is then mounted on the vacuum flange with electrical feed throughs and connected to the SMU on the outside.

2.2. Sample illumination

The AC, with the samples, is illuminated using the solar simulator. Inside the chamber the intensity is reduced

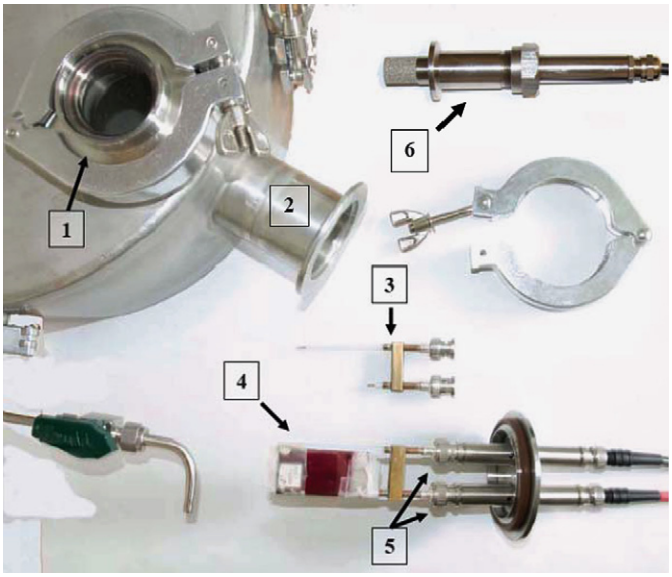

Fig. 5. Viewport for exposing the sample to light (1), KF flange for introducing the samples (2), holder with BNC connections for fixing the samples (3), tested solar cell (4), cell with holder fixed on the flange through BNC connections (5) and humidity sensor with high-grade steel housing (Gallatec) (6).

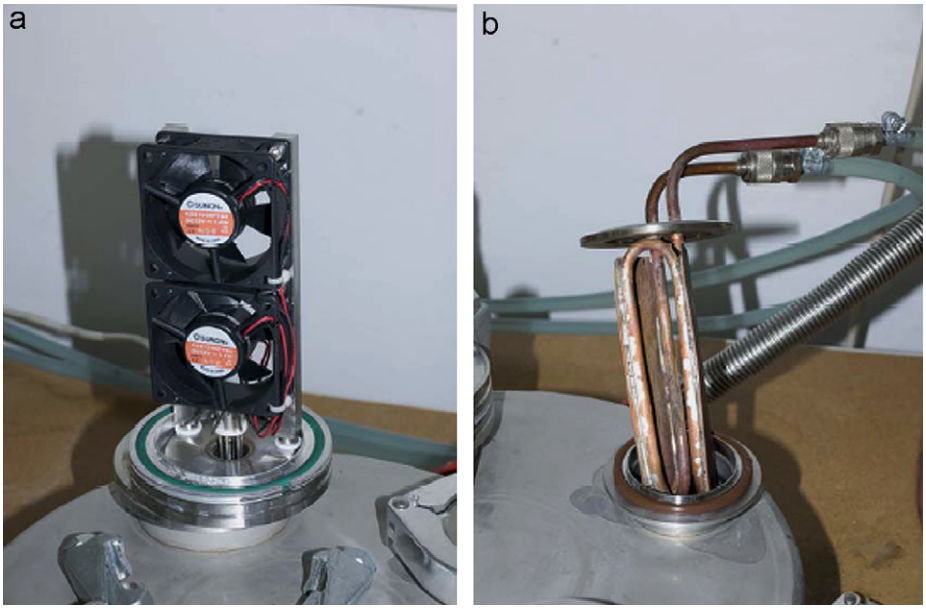

Fig. 4. System for circulation with two fans fixed on the flange (a) and the cooling copper pipe welded on the flange (b).

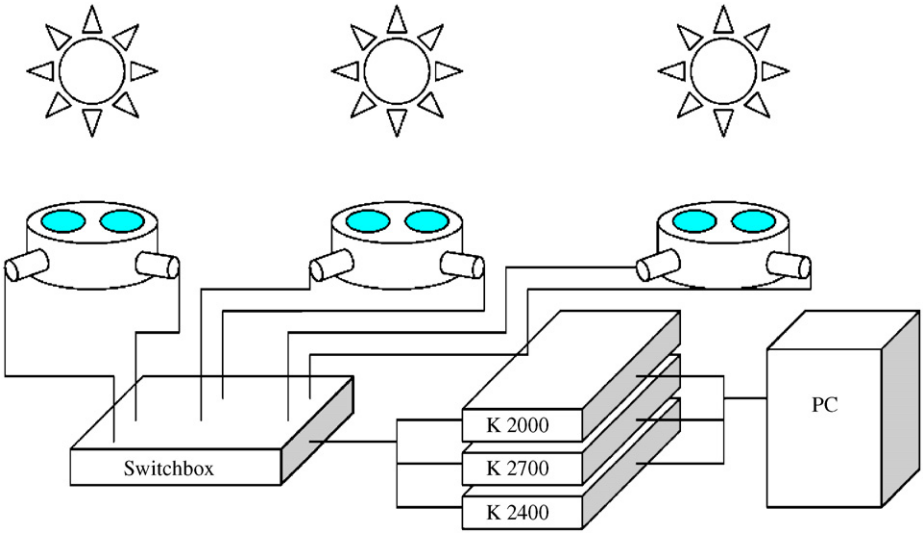

Fig. 6. Schematic drawing of the PC-controlled Keithley 2400 SMU and multiplexing unit Keithley 2700.

somewhat partly because a small part of the radiation is absorbed in the quartz windows, and partly because the window aperture is limited (inner diameter 36.4 mm) such that essentially only the direct light reaches the devices. If the outside lamp intensity is adjusted to 1 sun (1000 W m^{-2}, AM1.5G) then the measured intensity that the devices receive is only $\frac{1}{3}$ sun (330 W m^{-2}) as measured using a KG5 filtered Hamamatsu S1133 photodiode. Degradation of devices may depend on the wavelength of the radiation and optical filters can be placed above the quartz windows. UV-filters (Thorlabs inc., FGL400S) were used to exclude UV radiation below 400 nm from reaching the devices.

2.3. High-temperature version of the atmospheric chamber

It is sometimes desirable to test devices at elevated temperature to accelerate the degradation.

For this purpose a chamber was heated using a heating block while the external cooling fans were switched off. With the current setup that employs cooling water to remove heat in conjunction with external cooling fans and a heating block the accessible temperature range is 25–85 °C.

2.4. Complex system for lifetime measurements

A complex system for systematic *IV* data measurements has been developed for decay studies. The entire setup has three identical solar simulators with three ACs capable of measuring a total of six solar cells and three pyranometers or silicon diodes to monitor the light intensity changes. Lifetime measurements are performed by taking *IV* diode characteristics at short intervals for >1000 h. In principle this could be accomplished by assigning a source-measurement unit (SMU) to each of the cells and the pyranometers/silicon diodes. A more economic solution is to use one single SMU (a Keithley 2400) for all measurements and use a switchboard controlled by a Keithley 2700 unit equipped with a 7705 control module with 40 relays. The intensity of the lamps is measured using an empty slot on the switchboard, the Keithley 2700 and a multimeter (Keithley 2000). This multiplexing setup is shown schematically in Fig. 6 below.

A computer is used to control the multiplexing unit so that the individual cells are connected to the SMU at regular intervals by opening and closing appropriate relays. When the cells are not being measured, they are connected to a load, which in this case was a short circuit. Other options are open circuit, a resistor or an active load, e.g. with a bias voltage to apply an electrical stress to the cell. The layout of the switch matrix is shown in Fig. 7 and was chosen to minimize electrical interference. Other connection matrices can be made with 40 relays such that up to 10 channels are available with load switching but with increased electrical interference and possible cross-talk.

The SMU is also computer controlled to run the *IV*-curve where the current is measured as a voltage is sourced to the device in typical voltage steps of 10–20 mV from -1 to $+1$ V. Interfacing the computer with the instruments is accomplished through a general-purpose interface bus (GPIB). When the *IV*-curve is measured instead of just a single current and/or voltage at each data point it is possible to extract the the short-circuit current (I_{sc}), open-circuit voltage (V_{oc}), fill factor (FF) and maximum power point at each time step. Information relating to the different decay processes in the device can be extracted from the *IV*-curve. Separate files are created to hold each of these parameters as well as the individual files containing the *IV* measurements. The automated program also has options for notifying the user via electronic mail when the device efficiency falls below a certain threshold or if the sun simulator lamp should fail.

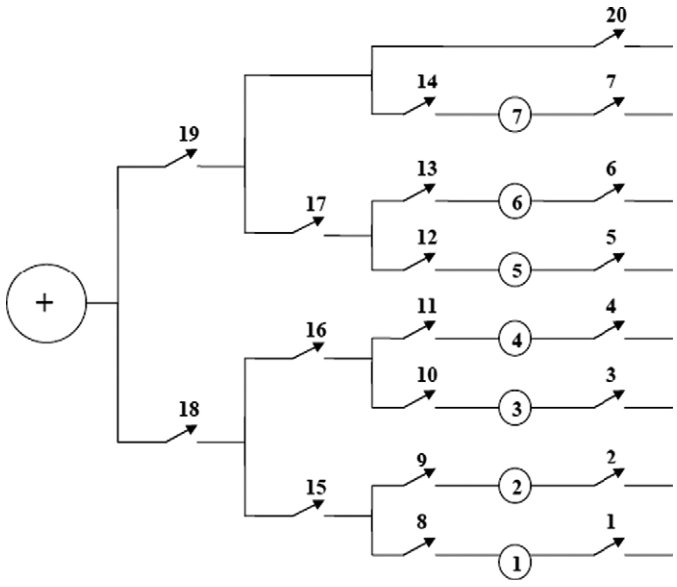

Fig. 7. The positive part of the switch matrix. The cells are marked as circles with numbers 1–7. Switches are marked 1–20. To measure cell 1 switches 8, 15 and 18 have to be closed to connect to the positive port of the SMU. Similarly, switches 28, 35 and 38 have to be closed to connect with the negative port of the SMU. Switches 1, 2, 3, 4, 5, 6 and 7 are connected to the load and are closed when the cell in question is not subject to measurements. The negative part of the switch matrix is not shown, but is otherwise identical to the positive switch matrix shown here.

2.5. Device preparation

A solution of PEDOT:PSS (Aldrich) was spin coated onto indium tin oxide (ITO)-covered glass slides (sheet resistance 8–12 Ω square^{-1}, Delta Technologies) and dried in an oven at (160 °C, 5 min). These substrates were then transferred to a glove-box environment where the active layer of P3HT/PCBM (1:1) (25 g mL^{-1} each in xylene) was spin coated. Finally, a layer of aluminum metal was evaporated on top. The final devices had an active area of 3 cm^2. All devices were subjected shortly to the ambient atmosphere for annealing at 150 °C for 6 min and characterization of the PV response. The solar cells were then mounted on holders (see Fig. 5) and placed inside the ACs (either in the atmosphere or in the glove-box environment). P3HT was prepared via the McCollough route [45] and the product had a regioregularity of 97% as established by 1H NMR. The polymer data were $M_w = 35\,600$, $M_n = 18\,700$, $M_p = 33\,900$, PD = 1.9.

3. Results and discussion

Eight lifetime experiments have been carried out in duplicate with the devices prepared above under ambient or nitrogen atmospheres at 25±1, 43±1, 63±1 or 83±1 °C. In the experiments with ambient atmosphere the humidity was measured to be 30±5% RH, while in the case of the nitrogen atmosphere the humidity was less than 0.1% RH and the oxygen level less than 2 ppm. The *IV* characteristics were recorded every 5 min for up to 200 h.

Table 1
Initial photovoltaic parameters for the glass/ITO/PEDOT:PSS/P3HT-[60]PCBM/Al devices employed here

Atmosphere	Temperature (°C)	V_{oc} (V)	I_{sc} (mA cm^{-2})	FF (%)	PCE (%)
Ambient	25±1	0.55	8.4	0.33	1.5
		0.55	7.8	0.31	1.3
	43±1	0.55	8.4	0.37	1.7
		0.55	8.2	0.33	1.5
	63±1	0.55	7	0.43	1.6
		0.57	6.5	0.47	1.7
	83±1	0.56	7.75	0.34	1.5
		0.55	8.1	0.32	1.4
Nitrogen	25±1	0.56	10.3	0.38	2.2
		0.56	10.5	0.37	2.1
	43±1	0.56	10.3	0.37	2.1
		0.56	10.6	0.36	2.1
	63±1	0.57	6.8	0.4	1.5
		0.55	6.9	0.44	1.6
	83±1	0.57	10	0.36	2.1
		0.56	10.6	0.35	2

The experiment at each temperature was performed for two independent cells. The device performance was recorded at and incident light intensity of 1000 W m^{-2}, AM1.5G, 72±2 °C, 35±5% relative humidity, ambient atmosphere. The active area of the devices was 3 cm^2.

From these data I_{sc}, V_{oc}, FF and relative power conversion efficiency (η) were calculated for each point in time.

Short circuit conditions were maintained while the devices were not being measured. The initial PV parameters varied somewhat between the devices as shown in Table 1. The major variation in the initial performance of the devices was in the short circuit current, whereas the V_{oc} was quite similar. We ascribe the small differences in V_{oc}, I_{sc}, FF and PCE to variations during device preparation and variation in film morphology.

The devices were subjected to continuous illumination at the specified temperature and atmosphere in the chambers. Devices operated in the ambient atmosphere degraded much faster than in inert nitrogen atmosphere as expected and also faster at higher temperature than at lower temperature.

In Fig. 8 the lifetime tests in the ambient atmosphere and in inert nitrogen at 43 °C are compared. The decay curves show a fast decay during the first few hours of testing and then stabilize to a constant decay that can be fitted with a linear or single exponential function. In this case where we employed relatively short test periods of a few hundred hours we chose a linear fit. The initial stabilization period could be due to an initial degradation mechanism involving the aluminum cathode that becomes less predominant after a short period of time. Since we observe it for cells tested in both ambient and inert atmospheres it could be linked to an oxidization of aluminum at the aluminum–polymer interface or it could be due to the reaction with water or oxygen introduced during initial testing. The curves obtained for the two devices in each test were more or less superimposable (not shown for clarity) with only slight variation indicating that the reproducibility of the

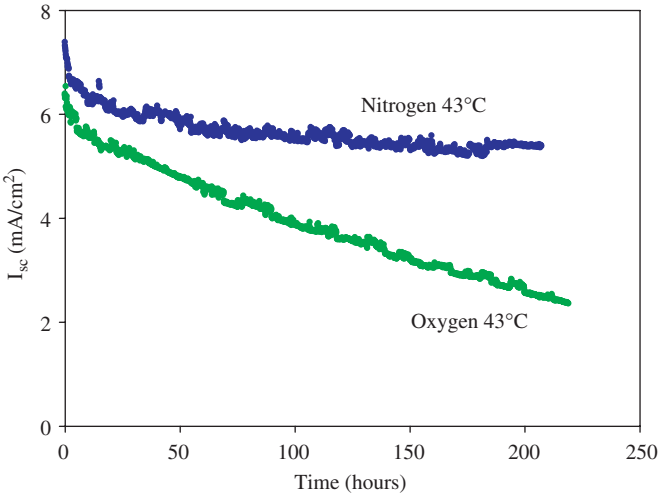

Fig. 8. Comparing the lifetime curves for devices in ambient atmosphere and in nitrogen at 43 ± 1 °C. The decay curves for the devices under the same conditions were quite similar and show a fast initial decay followed by region with a constant decay that can be fitted with a linear or an exponential function.

measurement of the decay curve was quite good. A reasonably fast decay was observed for the devices maintained in ambient atmosphere, which degraded to 50% of the initial performance after 150 h. A much slower decay was observed for the devices maintained in the nitrogen atmosphere that remained above 70% of the initial current after 200 h, which is consistent with earlier findings [46]. Similar relations between results in ambient atmosphere and nitrogen were seen also for other temperatures (25, 63 and 83 °C). The degradation of a PV device is characterized by a degradation constant that is obtained by fitting a suitable function to the decay curve for a device that shows the decay. The device current was chosen here and as mentioned above it can be fitted with either a linear (Eq. (1)) or a single exponential function (Eq. (2)). In our case the curves exhibit at least two regions where the rate of degradation is different. We chose the constant region observed after 15 h and fitted a linear function (Eq. (1)). Our reason for this is that it seems to be the typical constant behavior of the devices. Assuming that the degradation constant (k_{deg}) depends on the temperature (T) given by the Arrhenius equation (Eq. (3)), an acceleration factor (K) can be derived from Eq. (4) by fitting the values for k_{deg}. Fig. 9 shows acceleration factor (K) plotted against $1/T$ for both ambient atmosphere and nitrogen and the exponential fit to the calculated values. The calculated rate constants (k_{deg}) for each device, the acceleration factors and the activation energies are shown in Table 2

$$I_{sc}(t) = I_{sc}(t_0)(1 - k_{deg}t) \quad (1)$$

$$I_{sc}(t) = I_{sc}(t_0)\exp(-k_{deg}t) \quad (2)$$

$$k_{deg} = A\exp\left(\frac{-E_a}{k_B T}\right) \quad (3)$$

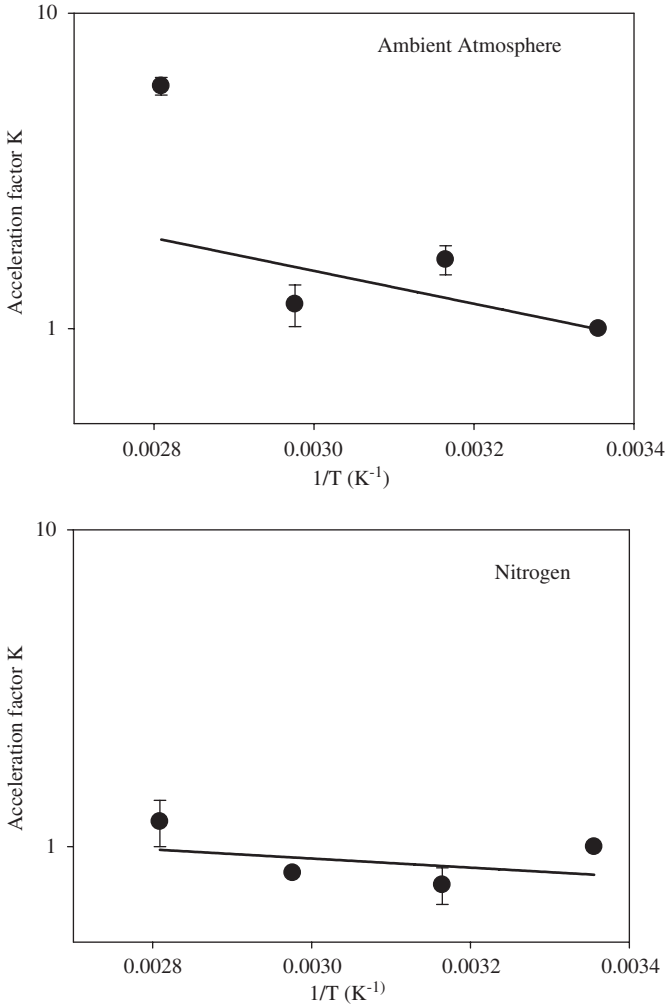

Fig. 9. Log scale plots of the acceleration factor, K, relative to 25 °C (298 K). The data were fitted using Eq. (4) and the parameters for the activation energy and the acceleration factor were obtained as shown in Table 2. The illumination intensity was $\frac{1}{3}$ sun (330 W m^{-2}).

$$K = \frac{k_{deg}(T_2)}{k_{deg}(T_1)} = \exp\left[\frac{E_a}{k_B}\left(\frac{1}{T_1} - \frac{1}{T_2}\right)\right]. \quad (4)$$

The activation energy has been extracted from the curves using Eq. (4) and in the case of ambient atmosphere it is rather low (103 meV), which might be due to fact that the data at 63 °C is an outlier. There is naturally a certain degree of experimental variation due to the fact that we could not prepare and run all eight experiments at the same time but had to run the experiments in three consecutive batches. The calculation of activation energy with omission of the point at 63 °C gives an activation energy that is 3 times higher than the one we obtain. This however underlines the difficulty in obtaining a value for the activation energy from one experiment and then generally applying it. Schuller et al. [43] performed accelerated measurements on devices based on MDMO-PPV and PCBM using both Ca/Ag and Al cathodes and obtained a value for the activation energy of 300–350 meV. This

Table 2
Rates of degradation, activation energy and acceleration constants obtained

Atmosphere	Temperature (°C)	k_{deg} (h^{-1})10^{-3}	K^a	E_a (meV)
Ambient	25±1	1.95	1	103
		0.96	1	
	43±1	2.16	1.48	
		2.67	1.83	
	63±1	1.7	1.17	
		1.78	1.22	
	83±1	8	5.5	
		9.1	6.25	
Nitrogen	25±1	0.92	1	29
		0.93	1	
	43±1	0.8	0.86	
		0.6	0.65	
	63±1	0.78	0.84	
		0.75	0.81	
	83±1	1.3	1.4	
		0.94	1.1	

[a] K was obtained by dividing each corresponding k_{deg} by average of k_{deg} values at 25 °C (except for values of K at 25 °C, which were simply normalized to one).

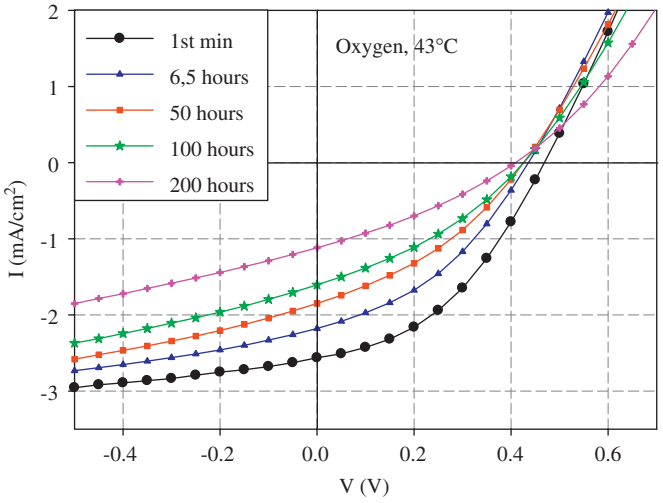

Fig. 10. Evolution of *IV*-curves during decay at 43 °C and ambient atmosphere (under $\frac{1}{3}$ sun illumination).

value was later employed by De Bettignies et al. [42] for a different polymer system P3HT to predict the operational lifetime under normal condition based on accelerated lifetime measurements. The lifetime under normal operational conditions was however not verified. In our case we employed the same material combination ITO, PEDOT:PSS, P3HT, [60]PCBM and aluminum. In our experiment we varied the light intensity, employed a UV-filter and did not have a LiF barrier layer between the active material and the cathode. Under inert conditions we obtain a totally different value for the activation energy and as a consequence a much slower acceleration factor indicating that there is no real acceleration of the degradation under inert conditions (albeit at lower light intensity and in the absence of UV-light). However, it is clear that the degradation proceeds much faster in the ambient atmosphere where oxygen and humidity are allowed to diffuse into the devices. This corroborates the results from several other studies on the degradation of polymer solar cell devices [16,20,42,43]. The degradation processes that take place in the presence of oxygen and humidity are most likely chemical processes involving the active polymer and perhaps the electrode materials. It is not so clear what causes the acceleration factor in our case to be much slower under nitrogen conditions. The limited data indicates that the process is not speeded up by increasing the temperature suggesting simple zero-order kinetics. This could happen if the rate of the process only depended on say the light intensity and not on the concentration and diffusion of molecular entities like oxygen and water. Further improvements to the setup would include the ability to increase and vary the light intensity in a larger range to investigate this issue.

The simple two-parameter exponential fit of the high-temperature degradation in ambient air does not describe the data completely. There seems to be two recognizable regions in the plot (Fig. 8): a rapid decrease in the first few hours followed by a more or less linear decay. This is consistent with earlier findings [17]. Using linear models for these two regions a better fit would of course be obtained in these regions and the acceleration factor would then be seen to change over time. The implications of this finding is that one has to exercise caution when estimating acceleration factors from decay curves that change over time as this may give rise to wrong estimates of operational lifetimes. Our results also strongly suggest that the determination and use of acceleration factors will only be applicable for one particular device constitution. This implies that even changing one constituent or interface layer is enough for the results not being useful. While we see accelerated studies as a useful means to characterize polymer and organic solar cells we also see it as limited to a particular device technology that cannot be extended to other systems without verification of the generality. The general degradation we observed for the devices were as expected with a decrease in mainly the I_{sc} but also the FF as the devices degraded as shown in Fig. 10 where the change of the *IV*-curve is shown for the devices maintained in ambient atmosphere at 43 °C.

As a further complication to the problem of obtaining an accurate stability measure for a given device technology we observed an unusual effect at the higher temperatures where atypical behavior sets in after a period of typically 50–100 h where a fast exponential decay was observed as shown in Fig. 11. At first we thought that this was due to a leak in the case of experiments studied under nitrogen but the observation was also made in ambient air. We currently have no explanation for this but consider this degradation path as a different one that is not linked to chemical changes in the material itself but perhaps to the macroscopic

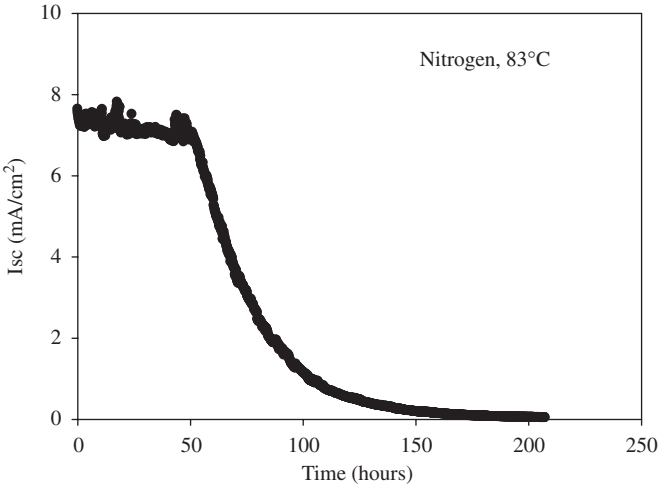

Fig. 11. Sudden fast decay behavior that we observed on occasion.

device. A likely explanation is incompatibility between the thermal properties of the individual layers in the multilayer device giving rise to a mechanical degradation.

Since we did not generally observe it and the onset of the fast degradation mechanism did not take place at a particular time we view it as a possible mechanical failure mechanism where the system delaminates or contact is lost between layers or at an interface. We did not include this behavior in the present study and only used the data that did not exhibit this behavior. We, however, chose to show the data here to underline the complexity of lifetime measurements and show that many processes may be in play that are not necessarily predictable.

4. Conclusion

An experimental setup for studying the lifetime and degradation of polymer solar cell devices has been described. This includes details of ACs that allow full control over the critical parameters that affect the decay of these devices with time. The setup consists of three ACs, where devices are connected to a single source meter through a computer-controlled switch matrix. Full *IV*-curves were recorded at 5-min intervals and the solar cell parameters of I_{sc}, V_{oc}, FF and η were extracted.

In the present paper the ACs and experimental setup were used to study the decay of ITO/PEDOT:PSS/P3HT-[60]PCBM/Al solar cell devices in ambient and nitrogen atmosphere at 25, 43, 63 and 83 °C. A rapid decay was recorded for the devices maintained in the ambient atmosphere with the presence of oxygen and water that could be fitted to a linear decay equation. An acceleration factor of about 6 was obtained by a ~60 °C increase in temperature. The decay mechanisms for devices maintained in ambient atmosphere can be ascribed to chemical reactions of the active layer and/or electrodes with oxygen and water that diffuse into the devices. The results from devices maintained in a nitrogen atmosphere showed that decay is much slower by more than one order of magnitude. What is more surprising is that no significant acceleration was found by increasing the temperature. The data are limited, but may suggest that the decay mechanism in this case is quite different, possibly only dependent on the light intensity or UV-light. The results also show that the decay of polymer solar cell devices is complicated and that several mechanisms operate. When the lifetime becomes sufficiently long it is not practical or possible to measure the whole decay curve until the devices are no longer operational. A few groups have resorted to accelerated tests where the temperature is increased to stress the devices and speed up the decay. The results in the present work show that the acceleration factor depends very much on the actual working conditions. It may also change value during the lifetime study if more than one mechanism is in operation. Accelerated studies may be necessary, but it is important that the exact experimental conditions are given; otherwise the results will be impossible to reproduce and interpret. Finally, results from accelerated lifetime testing cannot be viewed as generally applicable to other device geometries than the one tested as different materials and different device constitutions may give widely different responses to accelerated test conditions.

Acknowledgments

This work was further supported by the Danish Strategic Research Council (DSF 2104-05-0052 and DSF-2104-07-0022). Torben Kjær is acknowledged for technical assistance.

References

[1] C.J. Brabec, N.S. Sariciftci, J.C. Hummelen, Adv. Funct. Mater. 11 (2001) 15.
[2] H. Spanggaard, F.C. Krebs, Sol. Energy Mater. Sol. Cells 83 (2004) 125.
[3] K.M. Coakley, M.D. McGehee, Chem. Mater. 16 (2004) 4533.
[4] H. Hoppe, N.S. Sariciftci, J. Mater. Res. 19 (2004) 1924.
[5] S. Günes, H. Neugebauer, N.S. Sariciftci, Chem. Rev. 107 (2007) 1324.
[6] C. Winder, N.S. Sariciftci, J. Mater. Chem. 14 (2004) 1077.
[7] E. Bundgaard, F.C. Krebs, Sol. Energy Mater. Sol. Cells 91 (2007) 954.
[8] B.P. Rand, J. Genoe, P. Heremans, J. Poortmans, Prog. Photovoltaic Res. Appl. 15 (2007) 659.
[9] G. Li, V. Shrotriya, J. Huang, Y. Yao, T. Moriarty, K. Emery, Y. Yang, Nat. Mater. 4 (2005) 864.
[10] W. Ma, C. Yang, X. Gong, K. Lee, A.J. Heeger, Adv. Funct. Mater. 15 (2005) 1617.
[11] J.Y. Kim, K. Lee, N.E. Coates, D. Moses, T.–Q. Nguyen, M. Dante, A.J. Heeger, Science 317 (2007) 222.
[12] L.J.A. Koster, V.D. Mihailetchi, P.W.M. Blom, Appl. Phys. Lett. 88 (2006) 093511.
[13] M.C. Scharber, D. Mühlbacher, M. Koppe, P. Denk, C. Waldauf, A.J. Heeger, C.J. Brabec, Adv. Mater. 18 (2006) 789.
[14] M. Jørgensen, K. Norrman, F.C. Krebs 92 (2008) 696–724, this issue; doi:10.1016/j.solmat.2008.01.005.
[15] H. Neugebauer, C. Brabec, J.C. Hummelen, N.S. Sariciftci, Sol. Energy Mater. Sol. Cells 61 (2000) 35.

[16] K. Kawano, R. Pacios, D. Poplavskyy, J. Nelson, D.D.C. Bradley, J.R. Durrant, Sol. Energy Mater. Sol. Cells 90 (2006) 3520.
[17] F.C. Krebs, J.E. Carlé, N. Cruys-Bagger, M. Andersen, M.R. Lilliedal, M.A. Hammond, S. Hvidt, Sol. Energy Mater Sol. Cells 86 (2005) 499.
[18] M. Lira-Cantu, F.C. Krebs, Sol. Energy Mater. Sol. Cells 90 (2006) 2076.
[19] J. Alstrup, K. Norrman, M. Jørgensen, F.C. Krebs, Sol. Energy Mater. Sol. Cells 90 (2006) 2777.
[20] K. Norrman, F.C. Krebs, Sol. Energy Mater. Sol. Cells 90 (2006) 213.
[21] K. Norrman, N.B. Larsen, F.C. Krebs, Sol. Energy Mater. Sol. Cells 90 (2006) 2793.
[22] K. Norrman, J. Alstrup, M. Jørgensen, F.C. Krebs, Surf. Interface Anal. 38 (2006) 1302.
[23] M. Lira-Cantu, K. Norrman, J.W. Andreasen, F.C. Krebs, Chem. Mater. 18 (2006) 5684.
[24] C.W.T. Bulle-Lieuwma, W.J.H. van Gennip, J.K.J. van Duren, P. Jonkheijm, R.A.J. Janssen, J.W. Niemantsverdriet, Appl. Surf. Sci. 203 (2003) 547.
[25] C.W.T. Bulle-Lieuwma, J.K.J. van Duren, X. Jang, J. Loos, A.B. Sieval, J.C. Hummelen, R.A.J. Janssen, Appl. Surf. Sci. 231 (2004) 274.
[26] F.C. Krebs, K. Norrman, Prog. Photovoltaic: Res. Appl. 15 (2007) 697.
[27] K. Emery, C. Osterwald, Sol. Cells 17 (1986) 253.
[28] K. Emery, C. Osterwald, Current Topics in Photovoltaics, vol. 3, Academic, London, 1988 (Chapter 4).
[29] K. Emery, in: A. Luque, S. Hegedus (Eds.), Handbook of Photovoltaic Science and Engineering, Wiley, Chichester, UK, 2003 (Chapter 16).
[30] Standard IEC 60904-3, Measurement Principles for Terrestrial PV Solar Devices with Reference Spectral Irradiance Data, International Electrotechnical Commission, Geneva, Switzerland.
[31] Standard IEC 60904-1, Photovoltaic Devices, Part 1: Measurement of Photovoltaic Current–Voltage Characteristics, International Electrotechnical Commission, Geneva, Switzerland.
[32] ASTM Standard G159, Standard Tables for Reference Solar Spectral Irradiances: Direct Normal and Hemispherical on 37° Tilted Surface, American Society for Testing and Materials, West Conshocken, PA, USA.
[33] ASTM Standard G173, Standard Tables for Reference Solar Spectral Irradiances: Direct Normal and Hemispherical on 37° Tilted Surface, American Society for Testing and Materials, West Conshocken, PA, USA.
[34] Standard ASTM E948, Standard Test Method for Electrical Performance of Non-Concentrator Photovoltaic Cells Using Reference Cells, American Society for Testing and Materials, West Conshocken, PA, USA.
[35] C.R. Osterwald, Sol. Cells 18 (1986) 269.
[36] Standard ASTM E1021, Standard Test Methods for Measuring Spectral Response of Photovoltaic Cells, American Society for Testing and Materials, West Conshocken, PA, USA.
[37] Standard ASTM E1328, Standard Terminology Relating to Photovoltaic Solar Energy Conversions, American Society for Testing and Materials, West Conshocken, PA, USA.
[38] J. Rostalski, D. Meissner, Sol. Energy Mater. Sol. Cells 61 (2000) 87.
[39] J.M. Kroon, M.M. Wienk, W.J.H. Verhees, J.C. Hummelen, Thin Solid Films 403 (2002) 223.
[40] V. Shrotriya, G. Li, Y. Yao, T. Moriarty, K. Emery, Y. Yang, Adv. Funct. Mater. 16 (2006) 2016.
[41] E.A. Katz, S. Gevorgyan, M.S. Orynbayev, F.C. Krebs, Eur. Phys. J.: Appl. Phys. 36 (2006) 307.
[42] R. de Bettignies, J. Leroy, M. Firon, C. Sentein, Synth. Met. 156 (2006) 510.
[43] S. Schuller, P. Schilinsky, J. Hauch, C.J. Brabec, Appl. Phys. A 79 (2004) 37.
[44] http://www.valleydesign.com/pyrexpic.htm.
[45] R.D. McCullough, R.D. Lowe, M. Jayaraman, D.L. Anderson, J. Org. Chem. 58 (1993) 904.
[46] X. Yang, J. Loos, S.C. Veenstra, W.J.H. Verhees, M.M. Wienk, J.M. Kroon, M.A.J. Michels, R.A.J. Janssen, Nanoletters 5 (2005) 579.